Isatogens: Further Studies of Crystal Structure, Electron Density, and ^{13}C and ^{15}N NMR Spectra

David B. Adams, Malcolm Hooper,* and Alan G. Morpeth
School of Pharmaceutical and Chemical Sciences, Sunderland Polytechnic, Sunderland SR2 7EE
Eric S. Raper
School of Chemical and Life Sciences, Newcastle upon Tyne Polytechnic, Newcastle upon Tyne NE1 5ST
William Clegg
Department of Chemistry, University of Newcastle upon Tyne, Newcastle upon Tyne NE1 7RU
Barry Stoddart
Proctor and Gamble Research, Whitley Road, Benton, Newcastle upon Tyne NE12 9TS

The structures of 2-(pyrimidin-2-yl) (**1c**), 2-methoxycarbonylisatogen (**1d**), and 2-(1-ethylbenzimidazol-2-yl)isatogen (**1e**) have been determined by X-ray crystallography. The dihedral angle between the isatogen ring and the plane of the 2-substituent varies as 43° (**1c**), 15° (**1d**), and 48° (**1e**). The *transoid* arrangement of the isatogen O(1) atom and the pyridine-type nitrogen atom N(15), previously reported in (**1b**), is preserved in (**1e**) despite the increased steric effects arising from the ethyl group in this molecule. There are surprising variations in the lengths of the O(1)–N(1)–C(2)–C(3)–O(3) bonds in the isatogen moiety and the C(2)–C(10) bond, this last having very little double bond character. MNDO calculations using the experimental geometries show, as before, that the C(2) atom carries a negative charge and indicate that there is a strong stereoelectronic effect arising from the centres of highest electron density in the isatogen ring O(1) and the nitrogen atoms, N(11) and N(18) in (**1c**) and (**1e**), which are remote from each other. The energies of the LUMO and HOMO orbitals indicate that the reaction between these isatogens and dipolarophiles shows the same regioselectivity reported in an earlier paper. Natural abundance ^{15}N NMR spectra of isatogens are reported for the first time. The chemical shifts of the N(1) atom in the isatogens (**1a–e**) correlate negatively ($r = -0.96$) with ^{13}C shifts of the C(3) atom, providing further evidence of the highly polarizable nature of the five-membered ring in the isatogen system.

The authors have previously reported a detailed study of the structure and chemistry of 2-phenyl- and 2-(pyrid-2-yl)isatogen (**1a**, **b**), compounds which are the prototype molecules of

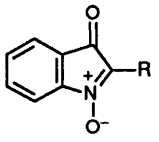

(1)

a; R = phenyl
b; R = 2-pyridyl
c; R = pyrimidin-2-yl
d; R = methoxycarbonyl
e; R = 1-ethylbenzimidazol-2-yl

a series of isatogens with interesting novel chemical and biological properties.[1] Of particular interest was the detailed geometry and electron densities of the O(1)–N(1)–C(2)–C(3)–O(3) isatogen moiety, the C(2)–C(10) inter-ring distances, and the dihedral angle between the two ring systems. The electron distribution in the isatogen ring is represented by the canonical forms I–IV in Figure 1. 2-Phenylisatogen has both rings almost coplanar whilst in 2-(pyrid-2-yl)isatogen the inter-ring dihedral angle is 45° (Table 1) with the two nitrogen atoms in a transoid arrangement. It was suggested that electrostatic repulsion between the negatively charged O(1) and O(3) atoms and the lone pair of electrons in the sp^2 hybridized orbital of the N(15) atom was responsible for the large dihedral angle, the *transoid* relationship of N(1) and N(15) being a consequence of the greater electron density on O(1) rather than O(3). It was decided to explore further these stereoelectronic effects by a study of the isatogens (**1c–e**). In 2-(pyrimidin-2-yl)isatogen (**1c**) the introduction of two nitrogen atoms into positions adjacent to the C(2)–C(10) bond would be expected to increase the stereoelectronic effect and consequently the dihedral angle between the two rings. In methyl isatogenate (**1d**) the sp^2 hybridized ester carbon atom would be expected to hold the electronegative oxygen atoms in equivalent positions to the pyrimidine nitrogen atoms, with similar consequences. In 2-(1-ethylbenzimidazol-2-yl) isatogen (**1e**) the steric demands of the ethyl group on the 'pyrrole-type' nitrogen atoms are in direct competition with the stereoelectronic demands of the lone pair of electrons on the 'pyridine-type' nitrogen atom of the imidazole ring. The earlier paper reported calculations of charge densities and HOMO and LUMO orbital coefficients, using the experimental geometries, which substantiated the analysis of structural features and rationalized some contradictory aspects of the chemistry of isatogens. The results of similar calculations for the isatogens (**1c–e**) are presented and discussed here. A further probe of the electronic effects occurring in the isatogen moiety are ^{13}C and ^{15}N chemical shift measurements. This paper reports new ^{13}C and ^{15}N NMR data and further structural and theoretical studies on the isatogens (**1a–e**), and an unambiguous assignment of the chemical shifts in (**1a**) which makes an important correction to those previously published.

Results and Discussion

Molecular Geometry.—The crystal structures of the isatogens (**1c–e**) are shown in Figures 2–4, with the corresponding bond lengths and angles listed in Tables 2–4 and torsion angles in

Table 1. Summary of major crystal features of isatogens (**1a–e**).

	(1a)	(1b)	(1c)	(1d)	(1e)
Bond lengths/Å					
N(1)–O(1)	1.261	1.280	1.245	1.248	1.260
N(1)–C(2)	1.372	1.350	1.476	1.374	1.354
C(2)–C(3)	1.430	1.451	1.411	1.429	1.454
C(3)–O(3)	1.232	1.223	1.239	1.228	1.226
C(2)–C(10)	1.456	1.449	1.476	1.462	1.448
Dihedral angle/°					
N(1)–C(2)–C(10)–X	7	45	43	15	48
Crystal cell	8(o)	8(o)	4(m)	4(t)	8(o)
Major intermolecular interactions	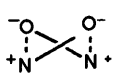	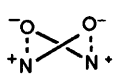			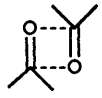

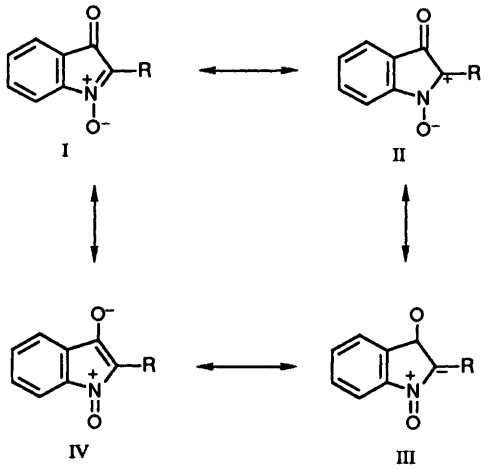

Figure 1. Canonical structures of isatogen moiety.

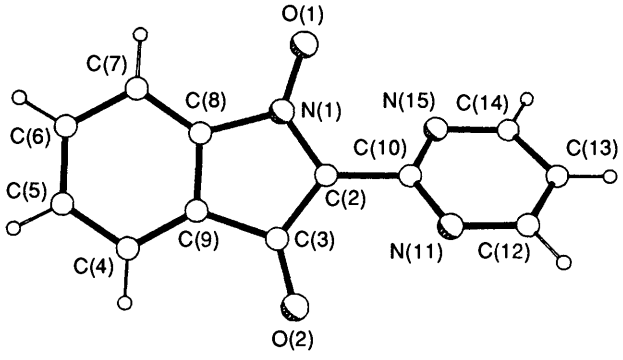

Figure 2. Crystal structure of 2-(pyrimidin-2-yl)isatogen (**1c**).

Table 5. Crystal-packing diagrams have been included in the deposited material. The similar bond lengths for C(8)–C(9), C(9)–C(3), and C(8)–N(1) and similar angles at C(8) and C(9) (Tables 2–4) indicate, as before, that the major changes in these molecules occur in the isatogen moiety. A number of interesting and surprising structural features can be identified. The pyrimidinyl isatogen (**1c**) (Figure 2) has an inter-ring dihedral angle of 43°, which is similar to that (45°) in 2-(pyrid-2-yl)isatogen (**1b**) (Tables 1 and 5). Compared with (**1b**) the N(1)–O(1) bond in (**1c**) has shortened and the C(3)–O(3) bond lengthened, making the isatogen moiety much more symmetrical, matching the symmetry of the pyrimidin-2-yl ring. A

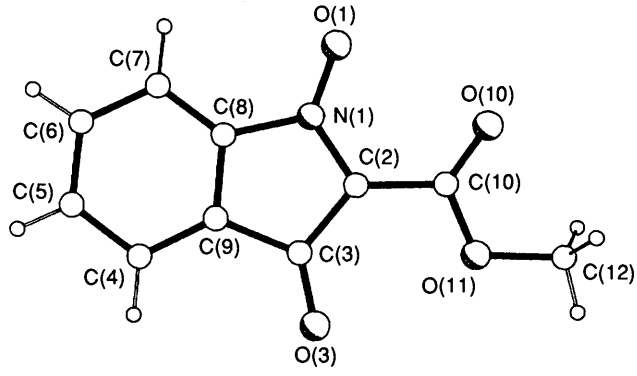

Figure 3. Crystal structure of 2-methoxycarbonylisatogen (**1d**).

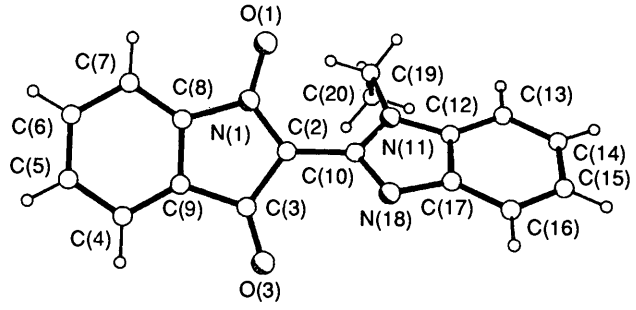

Figure 4. Crystal structure of 2-(1-ethylbenzimidazol-2-yl)isatogen (**1e**).

further noteworthy change in (**1c**) is the increased length of the C(2)–C(10) bond to 1.476 Å. This value approaches that of a single bond between two sp^2 hybridized carbon atoms in an α-dicarbonyl system of 1.49 ± 0.01 Å.[2] These changes are also reflected in the principal solid-state intermolecular interactions which involve head-to-tail associations between the N(1)–O(1) bond of one molecule and the C(3)–O(3) bond of another—a marked contrast with the crossed N(1)–O(1) interactions in (**1a**) and (**1b**) (Table 1).

In (**1d**) the molecule was, rather surprisingly, found to be almost planar (Figure 3) with an inter-ring dihedral angle through the C(2)–C(10) bond of only 15°, similar to that in (**1a**) (see Table 1). There was a shortening of the N(1)–O(1) bond but no compensating increase in the C(3)–O(3) bond length. The C(2)–C(10) bond distance was similar to that in (**1c**), increasing the distance between the isatogen ring and the ester side-chain (Table 1). A further surprising change, that could not occur in the cyclic system, was the extensive

Table 2. Bond lengths/Å and bond angles/° for compound (**1c**).

Bond lengths			
O(1)–N(1)	1.245(2)	N(1)–C(2)	1.377(2)
N(1)–C(8)	1.465(2)	C(2)–C(3)	1.411(2)
C(2)–C(10)	1.476(2)	C(3)–O(3)	1.239(2)
C(3)–C(9)	1.485(2)	C(4)–C(5)	1.390(3)
C(4)–C(9)	1.367(2)	C(5)–C(6)	1.377(3)
C(6)–C(7)	1.400(3)	C(7)–C(8)	1.365(2)
C(8)–C(9)	1.377(2)	N(11)–C(10)	1.325(2)
N(11)–C(12)	1.344(2)	C(10)–N(15)	1.322(2)
N(15)–C(14)	1.340(2)	C(14)–C(13)	1.376(3)
C(13)–C(12)	1.361(3)		
Bond angles			
O(1)–N(1)–C(2)	127.6(1)	O(1)–N(1)–C(8)	123.2(1)
C(2)–N(1)–C(8)	109.3(1)	N(1)–C(2)–C(3)	108.3(1)
N(1)–C(2)–C(10)	124.9(1)	C(3)–C(2)–C(10)	126.8(1)
C(2)–C(3)–O(3)	128.2(1)	C(2)–C(3)–C(9)	107.5(1)
O(3)–C(3)–C(9)	124.2(1)	C(5)–C(4)–C(9)	116.9(2)
C(4)–C(5)–C(6)	122.1(2)	C(5)–C(6)–C(7)	120.4(2)
C(6)–C(7)–C(8)	116.5(2)	N(1)–C(8)–C(7)	129.4(1)
N(1)–C(8)–C(9)	107.6(1)	C(7)–C(8)–C(9)	122.9(1)
C(3)–C(9)–C(4)	131.7(2)	C(3)–C(9)–C(8)	107.2(1)
C(4)–C(9)–C(8)	121.1(1)	C(10)–N(11)–C(12)	115.2(1)
C(2)–C(10)–N(11)	116.3(1)	C(2)–C(10)–N(15)	116.2(1)
N(11)–C(10)–N(15)	127.5(1)	C(10)–N(15)–C(14)	115.7(1)
N(15)–C(14)–C(13)	121.8(2)	C(14)–C(13)–C(12)	117.3(2)
N(11)–C(12)–C(13)	122.4(2)		

Table 3. Bond lengths/Å and bond angles/° for compound (**1d**).

Bond lengths			
N(1)–O(1)	1.248(3)	N(1)–C(2)	1.374(4)
N(1)–C(8)	1.452(3)	C(2)–C(3)	1.429(3)
C(2)–C(10)	1.462(4)	C(3)–O(3)	1.228(4)
C(3)–C(9)	1.479(4)	C(4)–C(5)	1.391(6)
C(4)–C(9)	1.383(3)	C(5)–C(6)	1.375(6)
C(6)–C(7)	1.379(4)	C(7)–C(8)	1.362(5)
C(8)–C(9)	1.377(4)	C(10)–O(10)	1.189(4)
C(10)–O(11)	1.317(5)	O(11)–C(12)	1.455(4)
Bond angles			
O(1)–N(1)–C(2)	128.2(2)	O(1)–N(1)–C(8)	121.7(3)
C(2)–N(1)–C(8)	110.1(2)	N(1)–C(2)–C(3)	107.7(2)
N(1)–C(2)–C(10)	122.1(2)	C(3)–C(2)–C(10)	130.2(3)
C(2)–C(3)–O(3)	128.4(3)	C(2)–C(3)–C(9)	107.0(3)
O(3)–C(3)–C(9)	124.7(2)	C(5)–C(4)–C(9)	116.1(3)
C(4)–C(5)–C(6)	121.4(3)	C(5)–C(6)–C(7)	122.1(4)
C(6)–C(7)–C(8)	116.3(3)	N(1)–C(8)–C(7)	129.9(3)
N(1)–C(8)–C(9)	107.4(3)	C(7)–C(8)–C(9)	122.7(2)
C(3)–C(9)–C(4)	130.8(3)	C(3)–C(9)–C(8)	107.8(2)
C(4)–C(9)–C(8)	121.4(3)	C(2)–C(10)–O(10)	123.6(4)
C(2)–C(10)–O(11)	112.4(3)	O(10)–C(10)–O(11)	124.1(3)
C(10)–O(11)–C(12)	115.2(2)		

shortening of the C(10)–O(10) double bond in the ester group to 1.189 Å. This very short distance corresponds to a carbon–oxygen bond with partial triple bond character, which varies from 1.207 ± 0.06 Å (conjugated systems) to 1.17 ± 0.1 Å (acyl halides, isocyanates).[3] Interestingly, the long (C2)–C(10) bond also indicates that there is little conjugation of this carbonyl group with the unsaturated system of the isatogen ring. The widening of the C(2)–C(10)–O(10) angle to 123.6° with a decrease in the C(2)–C(10)–O(11) angle to 115° contributes to the accommodation of the C(10)–O(10) carbonyl group in a *cisoid* position relative to the N(1)–O(1) bond. The intermolecular interactions in the crystal are also changed, the N–O bonds associating in a head-to-tail fashion in contrast to the crossed N–O bonds in (**1a**) and (**1b**) and the carbonyl/*N*-oxide interactions in (**1c**) (Table 1). Methyl isatogenate is an unstable molecule and readily decomposes into a mixture of products which have not been characterized. Jones and Kirby[4] have shown that bond stretching in the ground state is indicative of the preferred route of fission in subsequent reactions. Methyl isatogenate would therefore be expected to lose its ester group readily.

In the isatogen (**1e**) there is competition between the steric effects arising from the alkyl substituent on the 'pyrrole-type' nitrogen atom N(11) and the stereoelectronic effect associated with the lone pair of electrons on the 'pyridine-type' nitrogen atom N(18). It was initially intended to investigate a series of molecules in which the size of the alkyl substituent was varied (H, Me, Et, Pr^i, and Bu^t) but, in the event, the unsubstituted and the t-butyl compounds were not available by the synthetic methods employed and only the ethyl compound (**1e**) gave suitable crystals for X-ray studies. The crystal structure of (**1e**) (Figure 4) shows that the N(1)–O(1), C(3)–O(3), and C(2)–C(10) bonds are similar to those in 2-phenylisatogen (**1a**), although the inter-ring dihedral angle of 48° is similar to those in (**1b**) and (**1c**) (Tables 1, 4, and 5). The preferred transoid arrangement of O(1) and N(18) is a dramatic illustration of the dominance of stereoelectronic effects in 2-substituted isatogens, making the investigation of the t-butyl derivative worthy of further effort. It is also noteworthy that isatogens in which severe steric constraints arise from groups not possessing lone pairs of electrons on heteroatoms, *e.g.* 2-(2,6-dimethylphenyl)isatogen, have yet to be prepared; such steric effects are therefore by no means insignificant. The cisoid arrangement of the N(1)–O(1) bond and the ethyl group on N(11) in (**1e**) also influences the solid-state intermolecular interactions which now involve a head-to-tail arrangement of only the C(3)–O(3) bonds (Table 1).

MNDO Calculations.—These were carried out using the experimental geometries. The charge densities at the key sites [(**1a–e**): O(1)–N(1)–C(2)–C(3)–O(3), C(10); (**1c**): N(11), N(15); (**1d**): O(10), O(11); (**1e**): N(11), N(18)] are given in Table 6. Generally these are in agreement with the conclusions on the bond lengths in the preceding section: the more polarized bonds are longer than the less polarized bonds. In particular, the magnitude of the charge on O(1) varies according to the sequence (**1b**) > (**1a**) > (**1e**) > (**1c**) > (**1d**) whilst the N(1)–O(1) bond lengths vary in a similar, but not quite identical, manner: (**1b**) > (**1a**) > (**1e**) > (**1d**) > (**1c**). The variations in charge at O(3) [(**1a**) > (**1c**) > (**1d**) ≥ (**1b**) > (**1e**)] and the C(3)–O(3) bond lengths [(**1c**) > (**1a**) > (**1d**) ≥ (**1e**) ≥ (**1b**)] are also similar.

The HOMO–LUMO coefficients and orbital energies for the isatogen moiety of (**1c–e**), calculated as before, show the same trends as those reported for (**1a**) and (**1b**) (data not shown) and indicate the same susceptibility to nucleophilic attack at the 2-position and the same regiospecifity in reactions with dipolarophiles.

NMR Studies.—The authors' previous paper assigned the ^{13}C resonances on empirical grounds.[1] Here a careful study of these assignments using $^{13}C\{^1H\}$ coupled spectra is reported which confirms the original assignments with two exceptions: the C(2) and C(9) resonances were mutually misassigned. The $^3J_{CH}$ coupling for the quaternary carbon atoms in 2-phenylisatogen was measured using gated decoupling techniques with suppression of the protonated carbon signals[5] [Figure 5(*a–e*)]. The carbonyl carbon C(3) resonance at 186.93 ppm appears as the expected doublet coupling with H(4), J = 3 Hz [Figure 5(*a*)]. The C(10) resonance appears as a triplet, J = 7.6 Hz [Figure 5(*b*)], coupling with the equivalent

protons H(12) and H(14). The resonance at 122.4 ppm now assigned to C(9), exhibits a sharp pair of doublets, J = 3 and 7 Hz, due to coupling with the non-equivalent protons H(5) and H(7) [Figure 5(*c*)]. The C(8) resonance at 147.83 ppm also appears as a double doublet, J = 6.5 and 12 Hz, coupling with H(4) and H(6) [Figure 5(*d*)]. The loss of definition of this signal is consistent with the presence of the adjacent quadrupolar nitrogen atom. A similar but more extensive broadening of the C(2) signal at 132.11 ppm is also observed. In this case the expected triplet, arising from coupling with H(11) and H(15), appears as a broad (18 Hz) singlet [Figure 5(*e*)]. The remaining carbon atoms of the phenyl ring, C(11)/C(15), C(12)/C(14), and C(13), gave the expected triplet, doublet, and triplet signals—data not shown. Spin–lattice relaxation times, T_1, have also been determined[6] for (**1a**)[7] and support these new assignments.

Table 4. Bond lengths/Å and bond angles/° for compound (**1e**).

Bond lengths			
N(1)–O(1)	1.260(1)	N(1)–C(2)	1.354(2)
N(1)–C(8)	1.464(2)	C(2)–C(3)	1.454(2)
C(2)–C(10)	1.448(2)	C(3)–O(3)	1.226(2)
C(3)–C(9)	1.477(2)	C(4)–C(5)	1.391(2)
C(4)–C(9)	1.372(2)	C(5)–C(6)	1.372(2)
C(6)–C(7)	1.394(2)	C(7)–C(8)	1.366(2)
C(8)–C(9)	1.382(2)	N(11)–C(19)	1.472(2)
N(11)–C(10)	1.377(2)	N(11)–C(12)	1.377(2)
C(19)–C(20)	1.498(2)	C(10)–N(18)	1.318(2)
N(18)–C(17)	1.385(2)	C(16)–C(15)	1.382(2)
C(16)–C(7)	1.396(2)	C(15)–C(14)	1.405(2)
C(14)–C(13)	1.373(2)	C(13)–C(12)	1.396(2)
C(12)–C(17)	1.402(2)		
Bond angles			
O(1)–N(1)–C(2)	128.1(1)	O(1)–N(1)–C(8)	121.6(1)
C(2)–N(1)–C(8)	110.3(1)	N(1)–C(2)–C(3)	107.6(1)
N(1)–C(2)–C(10)	127.5(1)	C(3)–C(2)–C(10)	124.7(1)
C(2)–C(3)–O(3)	127.3(1)	C(2)–C(3)–C(9)	106.8(1)
O(3)–C(3)–C(9)	125.9(1)	C(5)–C(4)–C(9)	117.1(1)
C(4)–C(5)–C(6)	122.0(1)	C(5)–C(6)–C(7)	120.9(1)
C(6)–C(7)–C(8)	116.2(1)	N(1)–C(8)–C(7)	129.0(1)
N(1)–C(8)–C(9)	107.6(1)	C(7)–C(8)–C(9)	123.4(1)
C(3)–C(9)–C(4)	132.2(1)	C(3)–C(9)–C(8)	107.5(1)
C(4)–C(9)–C(8)	120.3(1)	C(19)–N(11)–C(10)	129.8(1)
C(19)–N(11)–C(12)	124.5(1)	C(10)–N(11)–C(12)	105.7(1)
N(11)–C(19)–C(20)	113.3(1)	C(2)–C(10)–N(11)	124.8(1)
C(2)–C(10)–N(18)	121.5(1)	N(11)–C(10)–N(18)	113.7(1)
C(10)–N(18)–C(17)	104.6(1)	C(15)–C(16)–C(17)	117.3(1)
C(16)–C(15)–C(14)	121.5(1)	C(15)–C(14)–C(13)	121.9(1)
C(14)–C(13)–C(12)	116.6(1)	N(11)–C(12)–C(13)	131.7(1)
N(11)–C(12)–C(17)	106.2(1)	C(13)–C(12)–C(17)	122.1(1)
N(18)–C(17)–C(16)	129.6(1)	N(18)–C(17)–C(12)	109.8(1)
C(16)–C(17)–C(12)	120.5(1)		

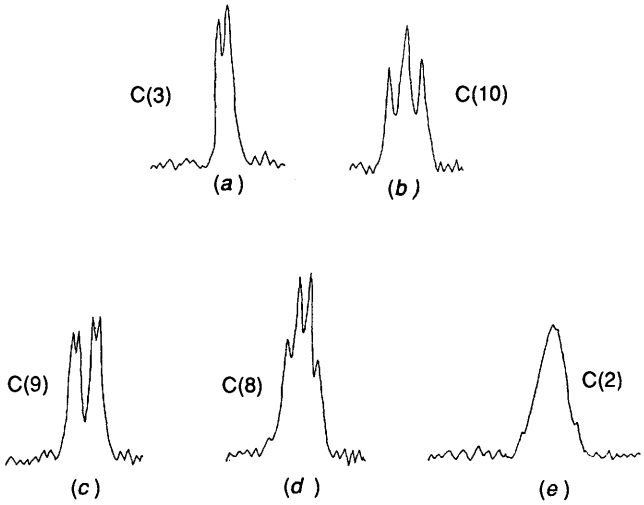

Figure 5. $^3J_{CH}$ coupling in phenylisatogen (**1a**): see text for chemical shifts and coupling constants.

Table 7. Chemical shifts in isatogens (**1a–e**).

	N(1)	C(2)	C(3)	C(10)
(**1a**)	−73.8	133.0	186.7	125.9
(**1b**)	−67.5	130.3	185.0	147.5
(**1c**)	−60.9	132.1	183.9	155.8
(**1d**)	−49.1	126.7	182.4	157.8
(**1e**)	−63.1	135.8	183.7	143.9

Table 5. Selected torsion angles/°.

Compound (**1c**)			
N(1)–C(2)–C(10)–N(11)	137.0(2)	C(3)–C(2)–C(10)–N(15)	137.4(2)
N(1)–C(2)–C(10)–N(15)	−43.1(2)	C(3)–C(2)–C(10)–N(11)	−42.5(2)
Compound (**1d**)			
N(1)–C(2)–C(10)–O(11)	−165.5(3)	C(3)–C(2)–C(10)–O(10)	−164.3(4)
N(1)–C(2)–C(10)–O(10)	14.4(6)	C(3)–C(2)–C(10)–O(11)	15.7(5)
Compound (**1e**)			
N(1)–C(2)–C(10)–N(18)	134.8(1)	C(3)–C(2)–C(10)–N(11)	137.1(1)
N(1)–C(2)–C(10)–N(11)	−48.2(2)	C(3)–C(2)–C(10)–N(18)	−39.9(2)

Table 6. Charges on key atoms for isatogens (**1a–e**).

Compound	O(1)	N(1)	C(2)	C(3)	O(3)	C(10)	N(11)	N(15)	N(18)	O(10)	O(11)
(**1a**)	−0.372	0.248	−0.121	0.311	−0.266	−0.027	—	—	—	—	—
(**1b**)	−0.392	0.250	−0.125	0.317	−0.235	0.080	—	−0.198	—	—	—
(**1c**)	−0.325	0.290	−0.164	0.316	−0.251	0.198	−0.229	−0.232	—	—	—
(**1d**)	−0.289	0.296	−0.256	0.325	−0.237	0.434	—	—	—	−0.301	−0.334
(**1e**)	−0.360	0.286	−0.149	0.315	−0.230	0.129	−0.165	—	−0.109	—	—

^{13}C and ^{15}N NMR studies. The relationship between charge density and chemical shifts is often contradictory, but it is generally agreed that the same factors influence both ^{13}C and ^{15}N chemical shifts.[8] However, in the latter case there are considerable differences between the reported chemical shifts which arise from the wide variety of experimental conditions used, particularly the selection of solvents and reference compounds.[8] We have measured the natural abundance ^{15}N chemical shifts in the isatogens (**1a–e**) under carefully controlled and identical conditions, and investigated the relationship between ^{15}N and ^{13}C chemical shifts (Table 7). When δ $^{15}N(1)$ was plotted against δ $^{13}C(3)$, a reasonably linear relationship was identified: $\delta C(3) = -0.17\,\delta N(1) + 173.76$; $n = 5$, $r = 0.96$. As the nitrogen signal becomes increasingly shielded the carbonyl carbon shift is affected in the opposite manner, becoming more deshielded. This is consistent with the high polarizability of the isatogen five-membered ring moiety and in agreement with the variations in charge density and the bond lengths noted above. However, there was no relationship between the calculated charge densities and the chemical shifts at these two centres. The correlations between N(1)/C(2), C(2)/C(10), and C(2)/C(3) chemical shifts were very much lower and not significant (r = 0.62, 0.53, and 0.42, respectively).

Attempts to design isatogen molecules with particular structural features thought to be associated with their interesting biological activities have led to some surprising results. Unpredictable changes in inter-ring dihedral angles, bond lengths and angles, and electron densities have been identified in all the compounds.

We are currently investigating two further series of isatogens designed on the one hand to generate large dihedral angles between the two ring systems and, on the other, to have increased conjugation of the isatogen ring with the 2-substituents.

Experimental

2-(Pyrimidin-2-yl)isatogen (**1c**).—2-Iodopyrimidine was prepared from 2-chloropyrimidine by treatment with hydriodic acid in 71% yield, m.p. 35 °C [light petroleum (b.p. 40–60 °C)] (lit., 36 °C[9]). The iodopyrimidine (32 mmol), 2-nitrophenylacetylene (32 mmol), bis(triphenylphosphine)palladium(II) dichloride (200 mg), and copper(I) iodide (80 mg) were refluxed under nitrogen in dry chloroform (100 cm^3) and dry triethylamine (10 cm^3) for 1 h, when TLC [silica gel; light petroleum (b.p. 60–80 °C)–ethyl acetate 3:2] showed the principal product, R_f 0.18, to be the required 1-(pyrimidin-2-yl)-2-(2-nitrophenyl)ethyne. The ethyne was obtained by Soxhlet extraction of the crude product adsorbed onto Celite–charcoal (5:1) using light petroleum (b.p. 40–60 °C) (43%) identified by the presence of a characteristic absorption band for a disubstituted acetylene at 2 220 cm^{-1}. Without further purification the ethyne (10.2 mmol) was heated under reflux for 40 h in chloroform (50 cm^3) containing nitrosobenzene (11.1 mmol). After removal of the solvent and nitrosobenzene under reduced pressure, the brown residue was recrystallized twice from ethanol to give the isatogen (**1c**) (1.09 g 46%), m.p. 209–210 °C (Found: C, 64.06; H, 3.06; N, 18.78. $C_{12}H_7N_3O_2$ requires C, 63.99; H, 3.13; N, 18.66%); ν_{max}(Nujol) 1 710 (CO), 1 570, and 1 445 cm^{-1} (pyrimidine ring); δ_H($CDCl_3$) 7.32 (t, 1 H, J 5 Hz, pyrimidine-H5), 7.78–7.59 (m, 4 H, aromatic hydrogens), and 8.97 (d, 2 H, J 5 Hz, pyrimidine-H4, -H6); δ_C($CDCl_3$) 114.86, 120.00, 121.00, 122.70, 132.10, 132.40, 134.60, 147.40, 155.78, 157.43, and 183.9.

2-(1-Ethylbenzimidazol-2-yl)isatogen (**1e**).—1-Ethyl-2-methylbenzimidazole was prepared by ethylation of 1-sodio-2-methylbenzimidazole to give a 99% yield of yellow oil, b.p. 130–134 °C/0.5 mmHg (lit., 187 °C/24 mmHg).[10] The benzimidazole (25 mmol) was converted first into 1-benzyloxy-1-phenyl-2-(1-ethylbenzimidazol-2-yl)ethene (72%) m.p. 127–129 °C, and then into 1-(1-ethylbenzimidazol-2-yl)-1-oximino-2-phenylglyoxal, 55%, m.p. 210–211 °C by the method of Albright and Shepherd.[11] The oximino compound (5 mmol) was treated with sodium nitrite (7.5 mmol) in phosphoric acid (15 cm^3, 88%) according to the method of Hagen *et al.*[12] The reaction mixture was poured into water, neutralized by the addition of potassium carbonate, and extracted with dichloromethane (4 × 100 cm^3). The combined extracts were washed with 10% sodium carbonate solution (3 × 50 cm^3) followed by water, dried (magnesium sulphate), and evaporated under reduced pressure. The crude product was purified by flash column chromatography [silica gel; eluant: light petroleum (b.p. 60–80 °C)–ethyl acetate 3:2], to give the isatogen (**1e**) (0.27 g 18%), deep-red needles (ethanol) m.p. 209–210 °C; ν_{max}(Nujol) 1 710 (CO), 1 480, 1 415, and 755 cm^{-1}. Elemental analysis was carried out as part of the X-ray crystallographic study. 2-Phenyl-, 2-(pyrid-2-yl)- and 2-methoxycarbonylisatogen (**1a, b, d**) were prepared in good yields by reported methods.[13a,b]

X-Ray Crystallography.—Crystal data. Compound (**1c**): $C_{12}H_7N_3O_2$, M = 225.21, monoclinic, a = 8.553(1), b = 7.246(1), c = 15.982(2) Å, β = 91.56(1)°, V = 990.12 Å^3 (by least squares refinement on 2θ angles for 30 reflections with 29 < 2θ < 35°), space group $P2_1/c$, Z = 4, D_c = 1.344 g cm^{-3}, F(000) = 464. Yellow–orange crystal, 0.27 × 0.27 × 0.30 mm, μ(Cu-K_α) = 0.85 mm^{-1}.

Compound (**1e**): $C_{17}H_{13}N_3O_2$, M = 291.31, orthorhombic, a = 24.725(2), b = 16.159 2(8), c = 6.975 9(3) Å, V = 2 787.2 Å^3 (from 32 reflections with 20 < 2θ < 30°), space group $Pbca$, Z = 8, D_c = 1.388 g cm^{-3}, F(000) = 1 216. Red crystal, 0.15 × 0.30 × 0.45 mm, μ(Cu-K_α) = 0.72 mm^{-1}.

Compound (**1d**): $C_{10}H_7NO_4$, M = 205.17, triclinic, a = 8.035(2), b = 8.094(2), c = 8.382(2) Å, α = 64.50(1), β = 71.35(1), γ = 70.57(1)°, V = 453.91 Å^3 (from 28 reflections with 20 < 2θ < 25°), space group $P\bar{1}$, Z = 2, D_c = 1.501 g cm^{-3}, F(000) = 212. Orange crystal, 0.35 × 0.35 × 0.08 mm, μ(Mo-K_α) = 0.11 mm^{-1}.

Data collection and processing. Siemens AED2 diffractometer, ω/θ scan mode, graphite-monochromated Cu-K_α radiation (λ = 1.541 84 Å) for (**1c**) and (**1e**), Mo-K_α radiation (λ = 0.710 73 Å) for (**1d**). Compound (**1c**): 2 234 reflections with 2$\theta \leqslant$ 155°, 2 014 unique (R_{int} = 0.074), 1 863 with $F > 4\sigma_c(F)$ (σ_c based on counting statistics only) after Lp and intensity decay corrections but no absorption corrections. Compound (**1e**): 5 304 reflections with 2$\theta \leqslant$ 155°, 2 805 unique (R_{int} = 0.033), 2 422 with $F > 4\sigma_c(F)$. Compound (**1d**): 2 874 reflections with 2$\theta \leqslant$ 50°, 1 599 unique (R_{int} = 0.027), 1 107 with $F > 4\sigma_c(F)$.

Structure Solution and Refinement.—Compound (**1c**): direct methods, blocked cascade refinement on F with anisotropic thermal parameters for non-H atoms and an empirical weighting scheme $w^{-1} = \sigma_c^2(F) + 2 + 14G + 4G^2 - 6S + 5S^2 - 16GS$ ($G = F_o/F_{max}$, S = sin θ/sin θ_{max}),[14] final R = 0.056, wR = 0.079, S = 1.41 for 155 parameters. All hydrogen atoms in calculated positions with C–H = 0.96 Å and U(H) = 1.2U_{eq}(C). Largest peak in final difference synthesis = 0.38 e Å^{-3}, largest hole = −0.26 e Å^{-3}. Scattering factors from 'International Tables,'[15] SHELXTL,[16] and local computer programs. Compound (**1e**) as for (**1c**), with w^{-1} = $\sigma_c^2(F) + 28 - 195G + 355G^2 - 65S + 39S^2 + 205GS$; R = 0.049, wR = 0.033, S = 1.46 for 203 parameters; largest peak = 0.30, largest hole = −0.18 e Å^{-3}. Compound (**1d**): $w^{-1} = \sigma_c^2(F) + 1 + 4G + 6G^2 - S + 2S^2 - 11GS$; R =

0.060, $wR = 0.039$, $S = 1.08$ for 140 parameters; largest peak = 0.24, largest hole = -0.42 e Å^{-3}.

Atomic co-ordinates are shown in Tables 9–11 of deposited material. Table 5 contains some relevant torsion angles for all three compounds. Labelled perspective diagrams are shown as Figures 2–4. The atomic co-ordinates for hydrogen atoms, anisotropic thermal parameters, and equations of least-squares mean planes have been deposited at the Cambridge Crystallographic Data Centre.* Packing diagrams are also included as Supplementary Material. The observed and calculated structure factors are available on request from the Editorial Office.

Calculations.—The MNDO calculations were performed using a redimensional version of the standard MNDO program[17] implemented on a Harris S100 computer at the computer centre, Sunderland Polytechnic.

NMR Spectra.—^{13}C *Spectra.* (*i*) The spectra of the isatogen (**1a**) were recorded on a JEOL GX-270 FT spectrometer operating at 67.80 MHz using deuteriochloroform as solvent and TMS as the internal standard. Digital resolution of 0.54 Hz was used for all spectra. 256 scans were obtained for the ^{13}C decoupled spectra; 512 scans were used for inversion recovery T_1 measurements utilizing a 25 s pulse delay; 4 000 scans were used for ^{13}C coupled spectra utilizing a 10 s pulse delay; 32 000 scans were used for ^{13}C coupled quaternary spectra, again with a 10 s pulse delay. (*ii*) The spectra of isatogens (**1a–e**) were recorded using a Bruker 300 MHz spectrometer operating at 75.00 MHz.

^{15}N *Spectra.* Natural abundance ^{15}N spectra of (**1a–e**) were recorded on a Bruker 300 MHz spectrometer operating at 30.42 MHz. 22 800–50 000 scans were accumulated using a pulse width of 12 s, using deuteriochloroform as solvent, $Cr(acac)_3$ as relaxing agent, and $Na^{15}NO_3$ as the external standard.

* For details of the CCDC deposition scheme, see 'Instructions for Authors (1990),' *J. Chem. Soc., Perkin Trans. 2*, 1990, issue 1.

References

1 D. B. Adams, M. Hooper, C. H. Swain, E. S. Raper, and B. Stoddart, *J. Chem. Soc., Perkin Trans. 1*, 1986, 1005.
2 'Handbook of Chemistry and Physics,' CRC Press, Boca Raton, Florida, 68th edn., 1987–88, p. F-160.
3 Ref. 2, p. F-161.
4 P. G. Jones and A. J. Kirby, *J. Chem. Soc., Chem. Commun.*, 1979, 288.
5 M. R. Bendall, *J. Chem. Soc., Chem. Commun.*, 1982, 1138.
6 R. L. Vold, J. S. Waugh, M. P. Klein, and D. E. Phelps, *J. Chem. Phys.*, 1968, **48**, 3831; R. Freeman and H. D. W. Hill, *ibid.*, 1969, **51**, 3140.
7 B. Stoddart and M. Hooper, *Magn. Reson. Chem.*, 1989, **27**, 241.
8 G. L. Nelson and E. A. Williams, *Prog. Phys. Org. Chem.*, 1976, **12**, 229; G. C. Levy, D. M. White, and F. A. L. Anet, *J. Magn. Reson.*, 1972, **6**, 453.
9 D. J. Brown and P. Waring, *Aust. J. Chem.*, 1973, **26**, 443.
10 Beilstein's 'Organische Chemie,' vol. 23, p. 145.
11 J. D. Albright and R. G. Shepherd, *J. Heterocycl. Chem.*, 1973, **10**, 899.
12 H. Hagen, R. D. Kohler, and E. H. Pommer, *Eur. Pat.* 54 147 (*Chem. Abstr.*, 1982, **97**, 216 185.)
13 (*a*) M. Hooper and S. P. Hiremath, *Adv. Heterocycl. Chem.*, 1978, **22**, 123; (*b*) C. C. Bond and M. Hooper, *J. Chem. Soc.* (*C*), 1969, 2453; (*c*) F. Krohnke and I. Vogt, *Chem. Ber.*, 1952, **85**, 368; (*d*) J. E. Bunney, Ph.D. Thesis, University of London, 1970; (*e*) H. E. Foster, unpublished data.
14 W. Hong and B. E. Robertson, in 'Structure and Statistics in Crystallography,' ed. A. J. C. Wilson, Adenine Press, New York, 1985, p. 125.
15 'International Tables for X-Ray Crystallography,' Kynoch Press, Birmingham, 1974, vol. 4, pp. 99, 149.
16 G. M. Sheldrick, 'SHELXTL, an integrated system for solving, refining and displaying crystal structures from diffraction data. Revision 5,' University of Gottingen, 1985.
17 M. S. J. Dewar and W. Theil, *J. Am. Chem. Soc.*, 1977, **99**, 4899, 4907.

Paper 0/00529K
Received 5*th February* 1990
Accepted 1*st March* 1990